JOURNAL OF CATALYSIS 127, 377–392 (1991)

Kinetic Studies of Catalytic Dehydration of *tert*-butanol on Zeolite NaH–ZSM-5

C. WILLIAMS,*,† M. A. MAKAROVA,* L. V. MALYSHEVA,* E. A. PAUKSHTIS,* E. P. TALSI,* J. M. THOMAS,† AND K. I. ZAMARAEV*

**Institute of Catalysis, Academy of Sciences Siberian Branch, Novosibirsk 630090, USSR; and †Davy Faraday Research Laboratory, The Royal Institution, 21 Albemarle Street, London W1X 4BS, United Kingdom*

Received March 22, 1990; revised July 25, 1990

Using a combination of FTIR spectroscopy and GC kinetic methods, we have studied in detail the adsorption and dehydration reaction of *tert*-butanol (*t*-BuOH) on H-ZSM-5. From FTIR studies of the kinetics of *t*-BuOH adsorption, we estimate the diffusion coefficient of *t*-BuOH in the zeolite channels as 5×10^{-11} cm^2s^{-1} at 23°C. The course of the dehydration reaction with time (in the temperature interval 23–60°C) is followed by simultaneous growth of a peak for adsorbed water, changes in the stretching and deformation vibrations for the adsorbed organic, and changes in the nature of the H-bonded species. These changes show that dehydration is accompanied by rapid isomerization and oligomerization of the butene product (the rates of isomerization and oligomerization substantially exceed the rate of dehydration), making it impossible to identify the intermediate for the dehydration reaction (be it carbonium ion or alkoxy species). Under reaction conditions the oligomers (most likely linear C_8 species) remain adsorbed on the active sites inside the zeolite channels, resulting in rapid deactivation of the sites. When the sites within the zeolite pores are completely deactivated, the dehydration reaction proceeds on sites located at the external surface of the zeolite crystallites. The latter sites are deactivated much more slowly than the former ones under our reaction conditions.

1. INTRODUCTION

Detailed experimental study of the mechanism of catalytic reactions at the molecular level is nowadays of crucial importance for both theoretical and applied catalysis (*1*). Catalytic reactions on zeolites are particularly suitable for such studies because of their uniform, ordered structure (*2*). Moreover, in these microporous, crystalline catalysts (with channels of molecular dimensions (*3*)), molecular diffusion may play an important role in the reaction, and experimentally determined diffusion coefficients may be used to further theoretical understanding of the molecular processes taking place on the catalyst surface.

We have chosen as a model reaction, the dehydration of *t*-BuOH on the acid form of zeolite ZSM-5. Alcohol dehydration on zeolites has received particular attention in the literature (*4*), not least because of the importance of the industrial methanol to gasoline process on H-ZSM-5 (*5*). In recent years, there have been attempts to identify reaction intermediates for alcohol dehydration by spectroscopic methods, namely IR (*6–8*) and ^{13}C NMR (*9–11*), with particular emphasis on distinguishing between the proposed carbonium ion type (A) and alkoxy type (B) intermediates:

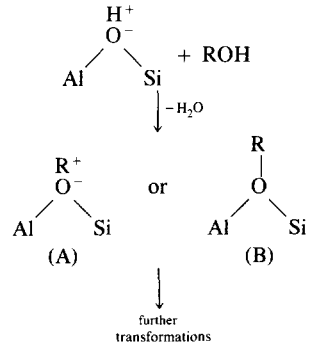

0021-9517/91 $3.00

Nevertheless, in our opinion, these studies have not been able to identify conclusively the reaction intermediate.

The dehydration of *t*-BuOH has received particular attention, since in classical organic chemistry terms, a tertiary species should give the most stable carbonium ion (*12*) and hence these carbonium ion species are more likely to be observed, if formed. Olah *et al.* (*13*) have reported evidence for the formation of stable *tert*-butyl carbonium ions in SbF_5 solution. More recently, spectroscopic studies of the nature of the adsorbed intermediate on dehydration of *t*-BuOH on H-ZSM-5 have been reported (*8, 10*). The adsorbed intermediate is considered to be stable *tert*-butyl carbonium ions of type A in Ref. (*8*), and a *tert*-butyl species more like the alkoxy species B in Ref. (*10*). Nevertheless, given the evidence of rapid oligomerization of olefins on acid zeolites (*14*), one should not exclude the possibility that the observed, adsorbed species may be oligomers as suggested in Ref. (*11*), which are secondary products of the dehydration reaction, rather than its intermediates.

As part of systematic kinetic and spectroscopic studies of dehydration of C_4 alcohols on H-ZSM-5, in the present work we concentrate on the dehydration of *t*-BuOH. We study the influence of diffusion control on the kinetics of this reaction and consider the complicating effect of secondary oligomerization of dehydration products. By comparing the rates of dehydration and oligomerization, we consider how possible it is to detect actual intermediates of dehydration.

2. EXPERIMENTAL

2.1. Materials

Three ZSM-5 samples were used for these studies; two of them, namely, samples 2 and 4, are designated as such since they were used in previous work (*15, 16*), and their relevant characteristics are summarized for convenience in Table 1, together with details for the new sample 5 (which was synthesized according to Ref. (*17*) with tetraethylammonium bromide as template.) The samples were converted into the acid (H^+) form via NH_4^+ ion exchange and calcination at 550°C. Samples 4 and 5 were fully exchanged, while sample 2, on which most of the work to be reported has been done, had 35% residual sodium ions. For one of these samples, namely sample 2, the concentration of Brønsted acid sites, [H^+], was determined using FTIR spectroscopy, ^1H NMR, pyridine poisoning experiments, and chemical analysis, as described elsewhere (*16*). The values obtained from these different methods were in reasonable agreement. For all the samples, the concentration of Lewis acid sites, determined by IR studies of CO adsorption as described in Ref. (*16*), was found to be less than 10% of the overall Al content. Therefore, for the other two samples, the concentration of Brønsted acid sites has been determined only by one method, namely chemical analysis, with the concentration of acid sites (OH-groups) being the difference between the concentration of Al and that of residual Na^+ cations. As shown previously (*15, 16*) in experiments with iso-butanol, it is these Brønsted acid sites (OH-groups), rather than Lewis acid sites, that serve as active centers for the dehydration reaction. Crystallite sizes were determined by scanning electron microscopy. Sample 2 has a rather broad particle size distribution (0.5–4 μm). These particles may perhaps be composed of aggregates of still smaller crystallites. Samples 4 and 5 had identical Si/Al ratios but different crystallite sizes; sample 4 had well-developed crystallites of 15–20 μm length, while sample 5 had

TABLE 1

Sample Characterization

Sample	Crystallite size (μm, SEM)	Si/Al	[H^+] ions/g[a]
2	0.5–4	20	3.3×10^{20}[b]
4	15–20	35	2.8×10^{20}
5	4–6	35	2.8×10^{20}

[a] Per gram of dehydrated sample.
[b] Na/Al = 0.35.

clusters (4–6 μm diameter) which may be composed of aggregates of smaller crystallites (see Figure 1). An aerosil sample (A-300, USSR) with a surface area of 300 m^2g^{-1} has also been used, as an inert sorbent for comparison with the zeolite. *Tert*-butanol (AR grade) was distilled and stored over molecular sieve to remove any remaining traces of water. All gases were dried over molecular sieves prior to use; the residual water content was below 10 ppm.

2.2 Apparatus

2.2.1 Kinetic GC studies. The dehydration reaction was studied in a flow microcatalytic reactor using a pelletized sample (0.3–0.5 mm size fraction) and a sample mass of typically 0.02 g; full details are given in Ref. (*16*). Briefly, the butanol was fed into the reactor as a gaseous mixture with helium (alcohol concentration typically 1.1 mol%, overall pressure 1 atm). The gas flow rate was typically 30–40 cm^3/min. The reaction was studied in the temperature range 40–60°C, and conversion was kept to <10%. Water, butene, and unreacted alcohol were analyzed by on-line gas chromatography. The reaction rate (in terms of butene and water evolution) is defined as

$$W(C_4H_8) = F \cdot [C_4H_8]/m$$

and

$$W(H_2O) = F \cdot [H_2O]/m,$$

where F is the helium–alcohol flow rate (cm^3/s), $[C_4H_8]$ and $[H_2O]$ are the butene and water concentrations, respectively (molecules/cm^3), and m is the sample mass (g).

2.2.2 Infrared (IR) studies. FTIR studies of the dehydration reaction were carried out in a thermostatted *in situ* IR cell on a Bruker FTIR spectrometer (IFS-113V). The construction of the IR cell is described in more detail in Ref. (*16*). The zeolite samples were pressed into self-supporting discs (mass typically 25 mg, ρ = 6–12 mg/cm^2). The tablets were calcined for 1 h in air and 2 h in vacuum (10^{-4} Torr) at 450°C (500°C in the case of aerosil). The sample was then cooled to the desired temperature and the IR spectrum of the dehydrated sample was recorded for reference purposes. The required amount of alcohol was then injected into the cell and the kinetics of adsorption and reaction were studied by following changes in the IR spectra with time. The amount of alcohol added was such that $[ROH]/[H^+]$ = 1.0. In these kinetic studies, spectra (of 10 scans each) can be collected every 25 s or so in the wavenumber interval 1200–4000 cm^{-1}. By plotting the difference between these spectra and the spectrum of the purely dehydrated sample, one can see the spectrum of the adsorbed species. For non-kinetic work, a typical number of scans was 200, with a resolution of 4 cm^{-1}.

3. RESULTS AND DISCUSSION

3.1 Interpretation of IR Spectra

Typical IR spectra after exposure to alcohol at room temperature are shown in Fig. 2 both for the zeolite sample 2 (Fig. 2a) and for aerosil (Fig. 2b). Here and below, these are difference spectra, subtracting the spectrum for the pure dehydrated sample of the same sorbent, which is used as a reference. Here there are peaks associated with the adsorbed organic species (alcohol or products of its reactions) and with the sorbent OH groups. The adsorbed organic species gives rise to three sets of peaks, namely those in the range 2800–3000 cm^{-1} (C–H stretching vibrations), those at ~1470 cm^{-1} and ~1380 cm^{-1} (C–H deformation vibrations), and a broader peak centered around 3500–3700 cm^{-1} (O–H vibrations of the alcohol) (*18*). The peak at ~1380 cm^{-1} has two components, viz. a very intense peak at 1375 cm^{-1} and a much weaker peak at 1394 cm^{-1} (these peaks being best resolved in the spectrum in Fig. 2b). This is characteristic of C–H deformations in a $(CH_3)_3C$– fragment (*18*) such as the one in *t*-BuOH. A weak shoulder to the 1470 cm^{-1} peak is observed at ~1440 cm^{-1} for room temperature adsorption on the zeolite, but this shoulder is absent at higher temperatures (see later).

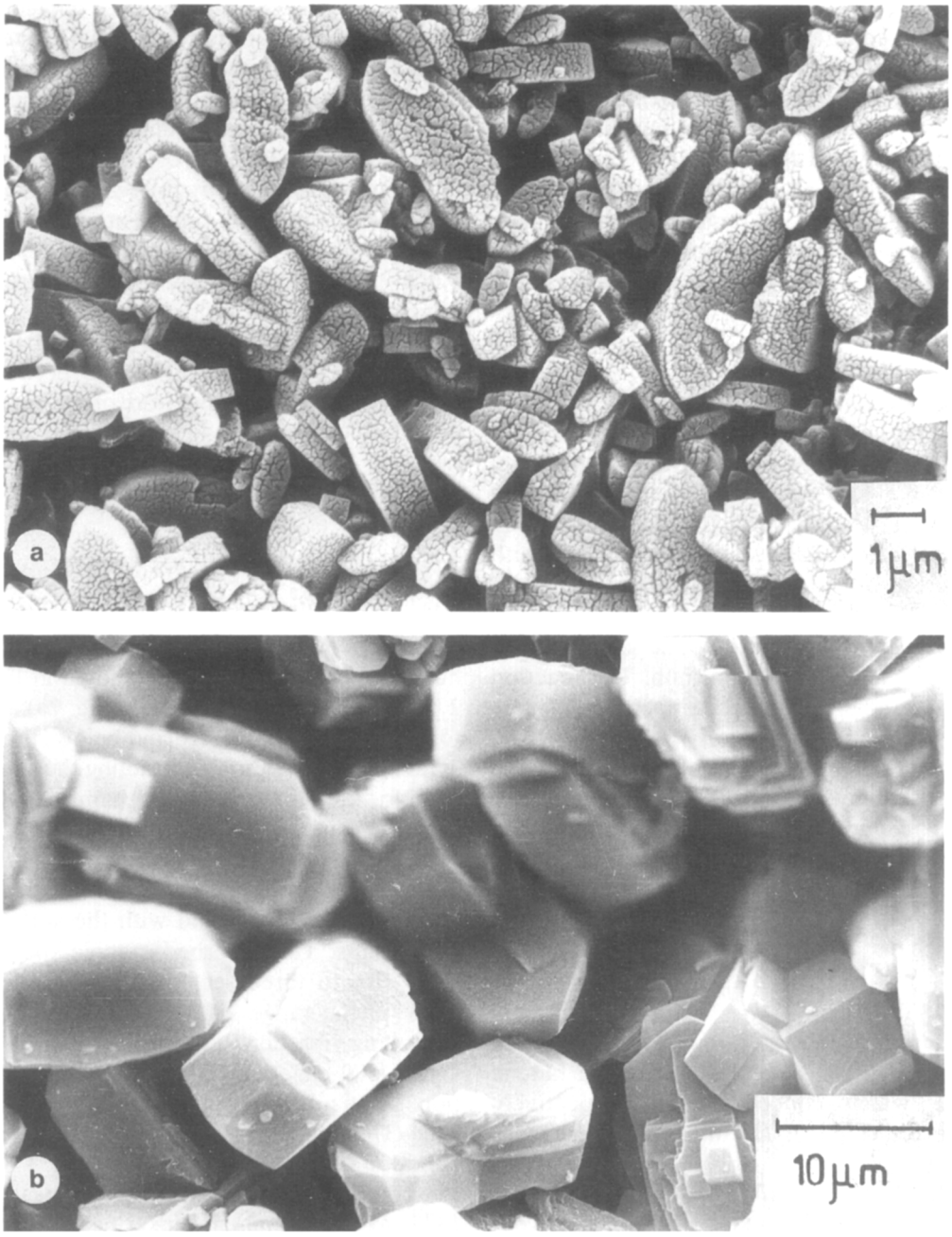

FIG. 1. Scanning electron micrographs for the ZSM-5 samples: (a) sample 2, 0.5–4 μm crystallites, which may be composed of aggregates of smaller crystallites; (b) sample 4, 15–20 μm crystallites; (c) sample 5, 4–6 μm crystallites, which may be composed of aggregates of smaller crystallites.

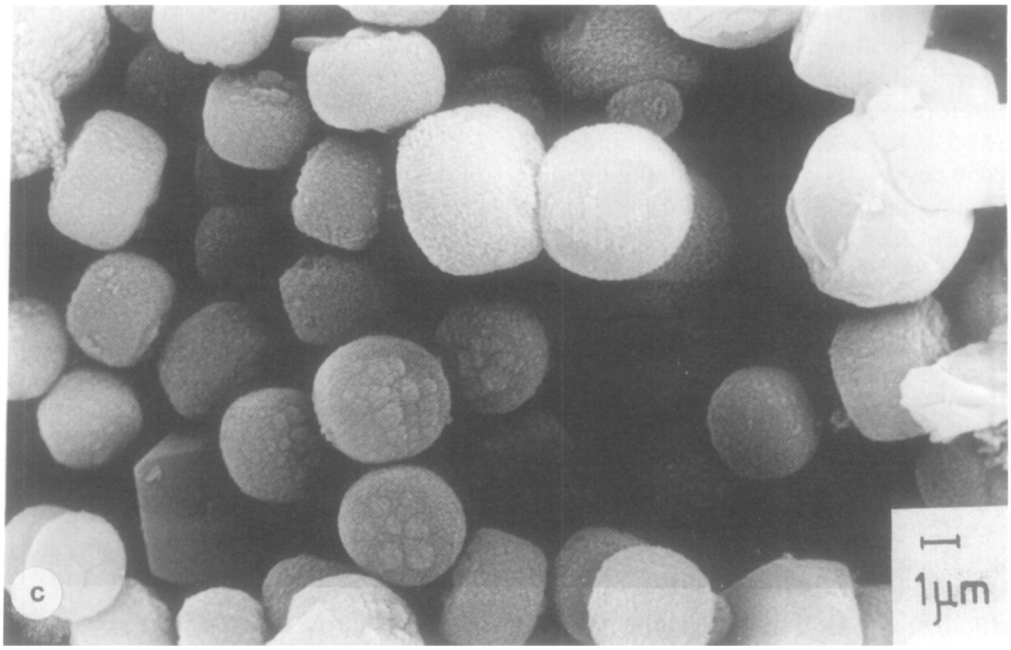

FIG. 1—*Continued.*

The peaks for the stretching vibrations of OH groups of the sorbents are observed as sharp "negative" peaks at 3740 cm^{-1} for terminal SiOH groups of aerosil (*19*) and at 3610 cm^{-1} for the acidic bridged OH groups in ZSM-5 (*20*). The negative peak shows the immediate decrease in the number of free OH groups in aerosil or zeolite on exposure to alcohol. In the case of aerosil, the SiOH groups weakly interact with *t*-BuOH, and the perturbed OH groups of aerosil give rise to a broad peak at ~3300 cm^{-1} (*19*). The alcohol molecules interact more strongly with the acidic OH groups of ZSM-5, giving rise to broad components at ~1500 cm^{-1} and ~2450 cm^{-1} for a H-bonded zeolite OH stretching vibration (*21*). Estimates of the integral intensities of these peaks suggest that practically all the OH groups are present in the form of H-bonded complexes.

In the case of aerosil, butanol does not undergo reaction, but for NaH–ZSM-5, an extra peak is observed at ~1640 cm^{-1}, corresponding to deformation vibrations of water molecules. The presence of this peak shows that even at room temperature, dehydration takes place to some extent. However, one should bear in mind that there may be sample heating in the initial few seconds after exposure to adsorbate (heat of adsorption effect), giving an apparent higher degree of reaction than would otherwise be

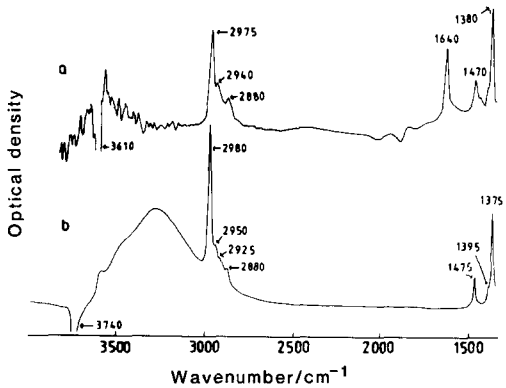

FIG. 2. IR difference spectra (subtracting the spectrum for the pure dehydrated sample) after exposure to *t*-BuOH at 23°C: (a) on ZSM-5 (sample 2) $t = 50$ s, and (b) on aerosil.

observed for a thermostatted sample at room temperature. Note also that the extent of reaction at room temperature is low. Therefore other peaks typical for the water/ZSM-5 system, i.e., broad components at ~2450 cm^{-1} (OH-groups of zeolite bonding to water) and 3690 cm^{-1} (OH-groups of water), are not observed in Fig. 2a because of their low intensity and overlap with the peaks at ~2450 cm^{-1} (OH-groups of zeolite bonded to alcohol) and 3500–3700 cm^{-1} (OH-groups of alcohol). However, these additional peaks involving water become clearly visible at higher extent of reaction (see later, Section 3.3.2, Fig. 4).

Let us now consider in more detail the characteristic deformation peaks at 1380 and 1470 cm^{-1}. The peak at 1380 cm^{-1} corresponds to the symmetric deformation vibration of $-CH_3$ fragments while that at 1470 cm^{-1} is in the region for deformation vibrations of both $>CH_2$ and $-CH_3$ fragments (*18*). For purely adsorbed *t*-BuOH, there will, of course, be no contribution to the 1470 cm^{-1} peak from the deformation in $>CH_2$ groups. However, if dehydration takes place, $>CH_2$ groups may be formed, and will contribute to the peak. Thus by monitoring the change in intensity of these two characteristic peaks, it should be possible to follow the change in concentration of CH_3 and $>CH_2$ fragments in the adsorbed species with time, i.e., one can follow the course of adsorption and reaction.

3.2 IR Studies of t-BuOH Diffusion

In order to find out whether the dehydration reaction is controlled by the diffusion of *t*-BuOH in the zeolite channels, we have followed, by means of IR spectroscopy, the uptake of *t*-BuOH on all three ZSM-5 samples at room temperature, 23°C (when the degree of reaction is expected, and was found, to be considerably reduced). Samples 4 and 5 have the same Si/Al ratio but different crystallite sizes, and sample 2 has Na^+ ions in addition to H^+ (Fig. 1, Table 1).

The results in Fig. 3 show the change in intensity of these two peaks with time for samples 4 and 5 (same Si/Al ratio and different crystallite sizes). Figure 3a shows the results for the 1470 cm^{-1} peak which, since it arises from deformation vibrations in both CH_3 and CH_2 groups, should be an indicator of the total amount of adsorbed organic species (alcohol or reaction products). The experimental data are displayed in terms of the kinetic dependence of the relative optical density

$$I_{1470} = D_{1470}/(D_{1470})_\infty,$$

where $(D_{1470})_\infty$ is the optical density of the difference peak after prolonged exposure, when adsorption is already complete.

For sample 5, there is a gradual growth in peak intensity during the first 2 min after exposure to alcohol; i.e., adsorption is taking place up to a saturation. Subsequently the peak intensity remains constant at this value of saturated adsorption. The increase in the 1470 cm^{-1} peak is accompanied by a simultaneous decrease in the intensity of the zeolite acid OH-peak at 3610 cm^{-1} (Fig. 3b), as more alcohol molecules diffuse into the bulk of the zeolite crystallites and adsorb onto the zeolite OH groups. For sample 4, on the other hand, a much more gradual growth in the peak intensity is observed with time. Thus the rate of adsorption is a function of crystallite size, being much slower for the 20 μm crystallites than for the 4–6 μm aggregates. This shows the diffusion nature of the adsorption kinetics.

At low sorbate concentrations, the uptake will be proportional to $t^{1/2}$ (*3*) and for our case of cubes of side, l, is described by

$$\frac{Q_t}{Q_\infty} = \frac{(D_{1470})_t}{(D_{1470})_\infty} = \frac{12}{l}\sqrt{\mathcal{D}t/\pi},$$

where Q_t and Q_∞ are the uptake at time t and at saturation, respectively, and $\mathcal{D}$ is the diffusion coefficient.

A plot of I_{1470} versus $\sqrt{t}$ for sample 4 is shown in Fig. 3c. It is seen to be close to linear. The fact that the straight line in Fig. 3c does not go through the origin may be the

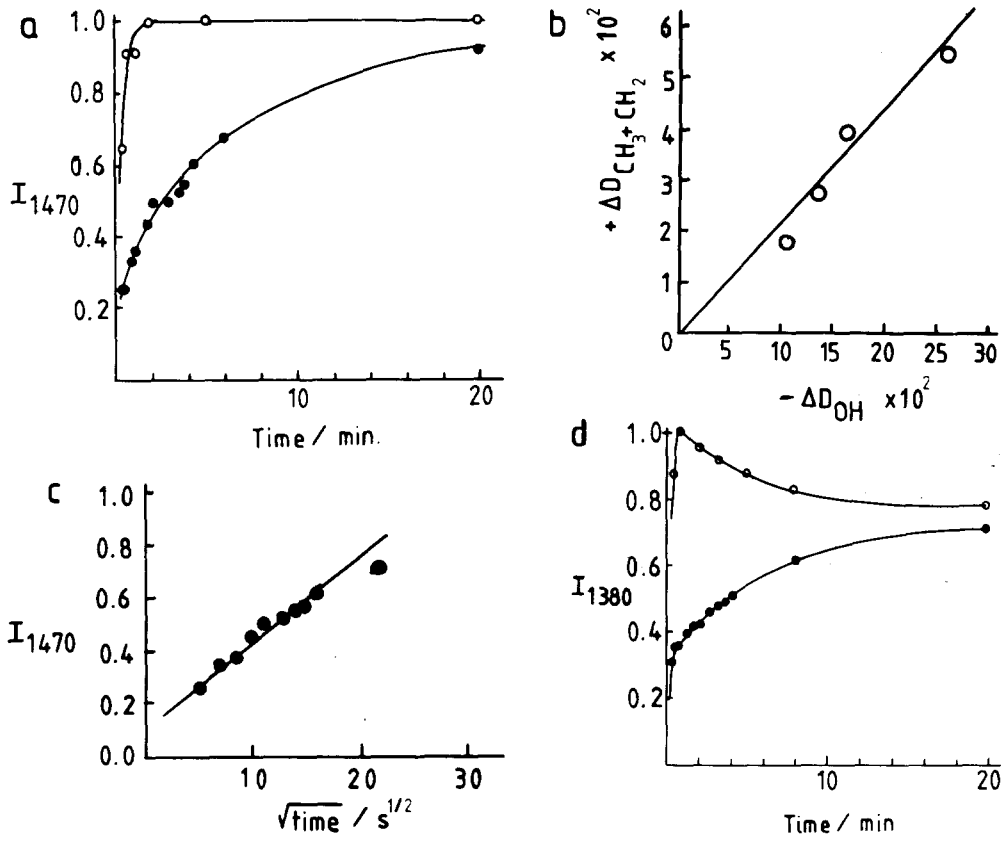

FIG. 3. IR spectroscopic studies of diffusion and reaction of *t*-BuOH on H-ZSM-5 at 23°C. (a) Change in intensity as a function of time after exposure to *t*-BuOH, for the 1470 cm^{-1} peak: (●) sample 4, (○) sample 5. This peak corresponds to deformation vibrations in both CH_3 and CH_2 organic fragments, and hence show the course of adsorption as function of time. (b) Decrease in the optical density of the zeolite OH-peak (3610 cm^{-1}) and the corresponding increase in the optical density of the CH_3 + CH_2 peak (1470 cm^{-1}), as adsorption proceeds, for sample 5. Eventually the zeolite OH-peak decreases to zero, showing that all the zeolite OH-groups are accessible to reactant. (c) Plot of I_{1470} versus $t^{1/2}$ for H-ZSM-5 sample 4. The estimated diffusion coefficient is $5 \times 10^{-11} cm^2 s^{-1}$. (d) Change in intensity as a function of time after exposure to *t*-BuOH, for the 1380 cm^{-1} peak. This peak corresponds to deformation vibrations in CH_3 groups only. (●) sample 4, (○) sample 5. Peak intensities, rather than peak areas are measured since there is no significant change in peak widths as a function of time. The actual function plotted in 3a and 3d is the relative optical density D/D_∞, normalized with respect to the optical density of the same peak after prolonged exposure, when adsorption is complete, and reaction has not taken place (see text for more details).

result of sample heating in the initial few seconds of adsorption, giving an apparent higher degree of adsorption than would otherwise be observed for a thermostatted sample at 23°C. From the observed linear dependence, the diffusion coefficient for *t*-BuOH in ZSM-5 channels can be estimated. Using the average crystallite diameter, *l*, given in Table 1, we obtain the following estimate:

$$\mathcal{D} = 5 \times 10^{-11}\ cm^2 s^{-1}$$

t-BuOH/H-ZSM-5/T = 23°C.

The obtained diffusion coefficient is reasonable in comparison with literature values (*22, 23*) for sorbate molecules of different sizes in H-ZSM-5. Thus:

$CH_4, H_2O \gg t\text{-}C_4H_9OH \simeq$ benzene, *p*-xylene

$10^{-5} - 10^{-6} cm^2 s^{-1}$ $\qquad$ $10^{-10} - 10^{-12} cm^2 s^{-1}$

Recently, Choudhary and Akolekar (*24*) referred to unpublished results for the diffusion coefficient of *tert*-butanol in H-ZSM-5, giving a value of $1 \times 10^{-12} cm^2 s^{-1}$, which again is in reasonable agreement with the values determined in the current work.

The results for the 1380 cm^{-1} peak are shown in Fig. 3d, using similar coordinates to those used in Fig. 3a, namely,

$$I_{1380} = D_{1380}/(D_{1380})_\infty,$$

where again $(D_{1380})_\infty$ is the optical density of the difference peak when adsorption is complete, and no reaction has taken place.

If the dehydration reaction were to take place, then taking the most simplistic view (ignoring for the time being complicating effects of isomerization and oligomerization), we have

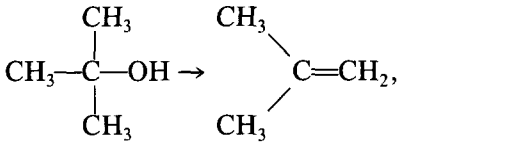

i.e., $3(CH_3) \rightarrow 2(CH_3) + (CH_2)$

Thus we see that on reaction, the number of CH_3 groups may decrease. This would give rise to a superposition of an increase in the number of CH_3 groups owing to adsorption, and a decrease in their number owing to reaction. In such a case, it is not possible to observe $(D_{1380})_\infty$ experimentally, and we must calculate it from the expression

$$(D_{1380})_\infty = (D_{1470})_\infty \cdot \frac{\varepsilon_{1380}}{\varepsilon_{1470}},$$

where $\varepsilon_{1380}/\varepsilon_{1470}$ is the ratio of the intensities of the respective peaks when no dehydration has taken place. Estimates for this ratio are obtained both for alcohol adsorbed on aerosil at room temperature (where no dehydration takes place, see Fig. 2b) and for the three ZSM-5 samples, taking peak intensities at $t = 25$ s (first point, and hence minimum degree of dehydration). Owing to the difference in peak widths for alcohol adsorbed on these different samples, peak area rather than peak height is used. The average value for this ratio is 3.6 ± 0.4. The error in this ratio gives rise to a systematic error of ca. 10% in the curves presented in Fig. 3d; this leaves the general form of the curves unchanged but means that the final peak intensity (at $t = 20$ min) is accurate only to ca. 10%.

In this case of purely adsorbed alcohol (and no reaction), the functions I_{1470} and I_{1380}, obtained in this manner, should be identical and should asymptotically approach 1.0. If we inspect the results in Fig. 3d, then for sample 5 we see that the peak intensity grows to 1.0 in the first minute after exposure to alcohol; this accompanies the increase in the 1470 cm^{-1} peak and shows increasing adsorption of alcohol onto the sample. Subsequently, the intensity of the 1380 cm^{-1} peak falls with time. Note that the peak at 1380 cm^{-1} from CH_3 groups is anomalously intense for CH_3 groups belonging to $(CH_3)_3C$-fragments. For example, the decrease in the intensity of this peak on going from *t*-BuOH or *i*-butane to, say, *i*-butanol, is considerably more than expected simply from the decrease in the number of CH_3 groups in the molecule (*18*). Thus the fall in intensity of the 1380 cm^{-1} peak in our case may result from the decrease both in the number of $(CH_3)_3C$-fragments and in the total number of CH_3 groups in the sample. The total number of $CH_3 + CH_2$ groups (1470 cm^{-1}), however, remains constant as suggested by Fig. 3a. Thus the decrease in the CH_3 peak is not caused by desorption of adsorbed species but rather from the dehydration reaction, resulting in a decrease in the amount of $(CH_3)_3C$-groups and the formation of water, as shown by the appearance and growth of the peak at 1640 cm^{-1} characteristic of adsorbed water (see Fig. 2a).

For sample 4, a much more gradual increase is observed in the intensity of the 1380 cm^{-1} peak, which accompanies the increase in the intensity of the 1470 cm^{-1} peak, and shows the slow adsorption of *t*-

BuOH. However, the intensity of the 1380 cm^{-1} peak at the end of adsorption for both samples 4 and 5 reaches only about 60–80% of the theoretically possible value. (That adsorption is complete for sample 5 and almost complete for sample 4 at $t = 20$ min is shown by the behavior of the 1470 cm^{-1} peak; see Fig. 3a.) This shows that for both samples reaction is taking place in addition to adsorption. However the difference between these two samples is that at 23°C, for sample 5 with smaller zeolite crystallites, adsorption proceeds notably faster than reaction, while for sample 4, the rates of adsorption and reaction are similar.

Thus by monitoring changes in the 1380 cm^{-1} and 1470 cm^{-1} peaks with time, it is possible to follow two processes:

(1) adsorption (resulting in $\uparrow CH_3$ and $\uparrow CH_2 + CH_3$

(2) reaction, with no product desorption (resulting in $\downarrow CH_3$ and no change in $CH_2 + CH_3$).

The relative rate of adsorption and reaction are different for samples 4 and 5. At room temperature for sample 5, adsorption is fast compared with reaction, while for sample 4, adsorption and reaction take place simultaneously. From these results, the importance of diffusion in *t*-BuOH dehydration on ZSM-5 becomes evident, as does the need for great care in kinetic work on this reaction, to ensure that experiments are not carried out in the region of diffusion control of the reaction.

3.3 IR Kinetic Studies of the Dehydration Reaction

3.3.1 Changes in the IR spectra with time. We have already observed in Section 3.1 that dehydration takes place to some extent even at room temperature. By recording IR spectra at higher temperatures, we study the course of reaction (rather than adsorption) in more detail. For this we have chosen sample 2, with small crystallite sizes in the range 0.5–4 μm. The IR spectra showing the course of reaction at 60°C, are presented in Fig. 4. Again, difference spectra are plotted,

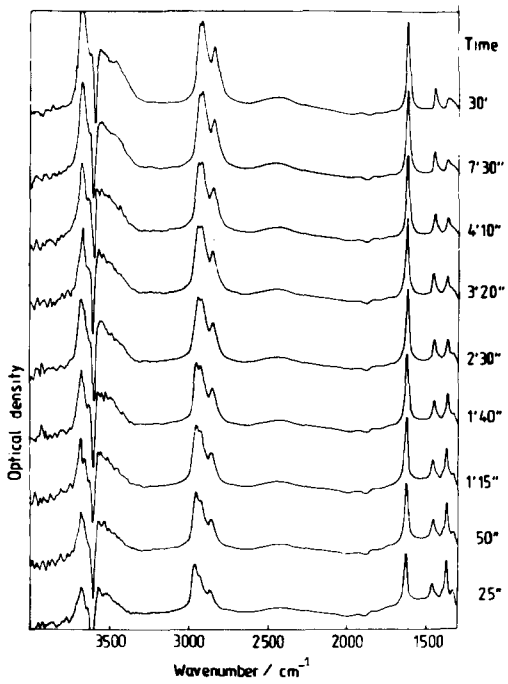

FIG. 4. IR difference spectra for sample 2 (subtracting the spectrum for the pure dehydrated zeolite), showing the course of reaction as a function of time after exposure to *t*-BuOH at 60°C.

subtracting the spectrum for the purely dehydrated zeolite. The main features for the first spectrum (25 s after exposure to alcohol) are rather similar to those for adsorbed alcohol at room temperature (Fig. 2a, Section 3.1), but with a more intense water deformation band at 1640 cm^{-1}, which increases with time, and eventually levels off. Comparing the water peak intensities, we see that $(I_{0.5min}/I_{30min}) = 0.5$; i.e., the dehydration reaction takes place rapidly, with approximately 50% reaction in the first 30 s. Concerning the peaks arising from the deformation vibrations of the organic fragments, then they are now situated at 1460 cm^{-1} ($CH_3 + CH_2$) and 1375 cm^{-1} (CH_3); they are slightly shifted from the positions noted in Section 3.1 owing to the much greater degree of reaction.

As time increases, changes are observed in the positions and/or intensities of peaks at 2800–3000 cm^{-1}, 1460 cm^{-1}, and 1375

cm^{-1} corresponding to organic fragments, and at ~2450 cm^{-1} and ~1500 cm^{-1} corresponding to H-bonded OH-groups of the zeolite (Fig. 4). The changes in peak intensities for the 1460 and 1375 cm^{-1} organic peaks and the 1640 cm^{-1} peak for water, during reaction at 40 and 60°C are shown in Figs. 5a and 5b. Thus for reaction at 60°C, the 1460 cm^{-1} peak increases rapidly with time, reaching 90% of its final value in the first minute after exposure to alcohol. This shows that adsorption of *t*-BuOH is practically completed by that time. The 1375 cm^{-1} peak decreases with time, in parallel with the growth of the 1640 cm^{-1} peak for adsorbed water. However, there is no corresponding decrease in the 1460 cm^{-1} peak; i.e., the amount of adsorbed organic remains constant and no organic reaction products desorb. The IR spectra show no peak characteristic of unsaturated olefins. The ν(C=C) peak typically at 1660–1670 cm^{-1} for butene isomers could be masked by the peak at 1640 cm^{-1} for adsorbed water. However, there should be no difficulty in observing the peak for ν(=C—H) which for butene isomers is in the region 3020–3090 cm^{-1} (*18*). Thus dehydration takes place (as seen by the growth of the water peak) but since the so-formed butene neither desorbs nor remains in the zeolite as a free or H-bonded olefin, the adsorbed organic species must be present as saturated rather than unsaturated hydrocarbon fragments.

3.3.2 Oligomers as proposed products. It has recently been proposed that the adsorbed organic species observed on dehydration of *t*-BuOH on H-ZSM-5 are stable *t*-butyl carbonium ions (*8*) or *t*-butyl silyl ethers (*10*). However, on the basis of our IR studies and GC kinetic studies (see later), we believe that the prevailing organic species present are saturated oligomers (most likely C_8 species) adsorbed on the active sites (octyl silyl ethers). We look in more detail at the evidence supporting this suggestion.

As time increases, we observe an increase in the 1640 cm^{-1} band (increasing dehydration), which is accompanied by a parallel and proportional decrease in I_{1375} ($(CH_3)_3C$-groups) in the absence of product desorption. This is shown in Fig. 5a and 5b for reaction at 40 and 60°C, respectively. The proportionality is shown more clearly in Fig. 5c, where the decrease in the intensity of the 1375 cm^{-1} peak (denoted $-\Delta D_{CH_3}$ is plotted against the increase in intensity of the water peak at 1640 cm^{-1} (denoted $+\Delta D_{H_2O}$) for all three reaction temperatures. As previously noted, the 1375 cm^{-1} peak from CH_3 groups is anomalously intense when these groups belong to $(CH_3)_3C$-groups. Thus the decrease in I_{1375} on dehydration of *t*-BuOH may have contributions both from the decrease in overall concentration of CH_3 groups and from their transfer from $(CH_3)_3C$-fragments to some other organic fragments. As a result, the decrease in peak intensity with time reflects the course of reaction, but the percentage change at any given time cannot be used to determine the percentage decrease in concentration of CH_3 groups, since ΔI is not necessarily linear in $[CH_3]$. But in any case, the results in Fig. 5 show that dehydration is accompanied by a substantial decrease in the number of $(CH_3)_3C$-fragments in the adsorbed organic species. This certainly suggests that tertiary butyl species (regardless of whether they are carbonium ion or alkoxy type in nature), are unlikely to be the prevailing adsorbed organic species observed during the reaction, since such species would give rise to the same number of $(CH_3)_3C$-fragments as in the original *t*-BuOH molecule.

This is further supported by the changes that we observe in the ν(C–H) region as time increases. Initially we observe three peaks at 2980, 2950, and 2890 cm^{-1}. As time increases, there is a growth in the central component and a shift in peak positions, so that after 2–3 min, the peaks are at 2960, 2940, and 2870 cm^{-1}. For the original *t*-BuOH, with only CH_3 groups, there should theoretically be only two peaks, typically at 2980–2960 cm^{-1} (asymmetric C–H stretch) and 2860–2890 cm^{-1} (symmetric C–H

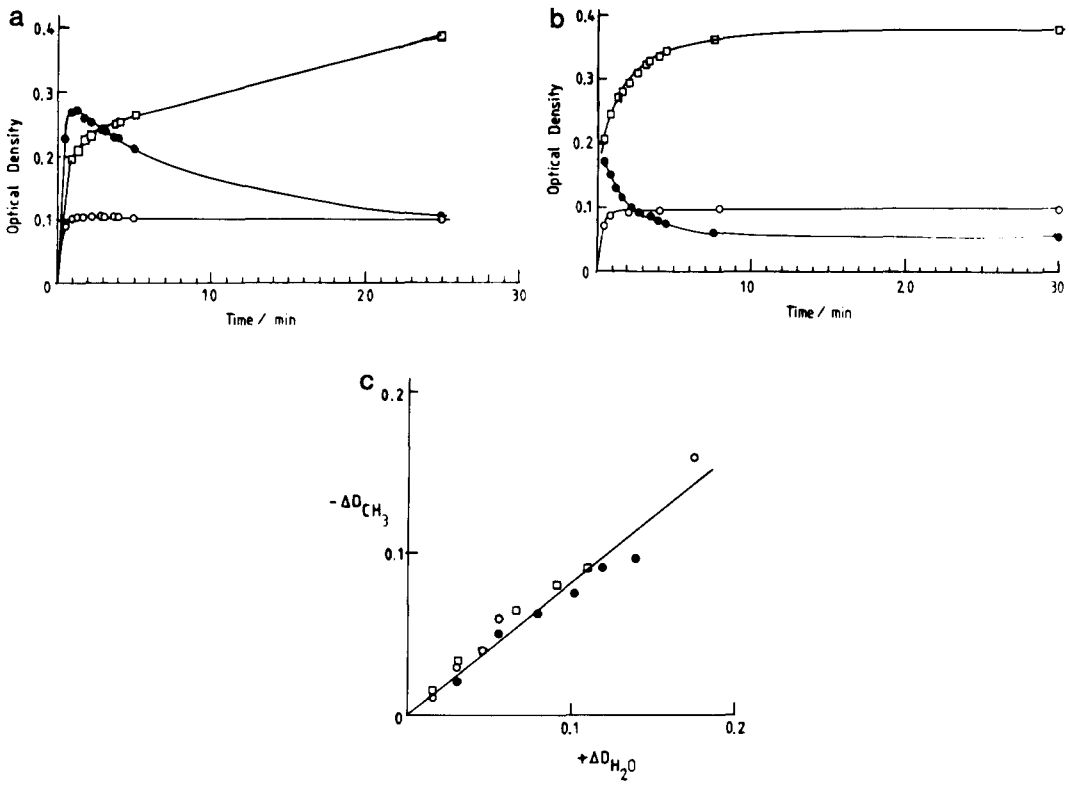

FIG. 5. Changes in intensities of the peaks at 1460 cm^{-1} (○), 1375 cm^{-1} (●), and 1640 cm^{-1} (□) as a function of time, in the course of reaction in the temperature range 23–60°C, for sample 2: (a) reaction at 40°C; (b) reaction at 60°C; (c) $-\Delta D_{CH_3}$ versus $+\Delta D_{H_2O}$ from IR spectra of reaction at all three temperatures 23°C (□), 40°C (○), 60°C (●). $\Delta D = D_t - D_{t_0}$, where t_0 is the time at which adsorption is complete, as determined from the intensity of the peak at 1460 cm^{-1}. t_0 has values of 50, 75, and 180 s for reaction at 60, 40, and 23°C, respectively.

stretch), but in all experimental spectra, a third peak in between these two is also observed and is usually assigned to an overtone (*18*). However, CH_2 groups also give rise to two peaks in this region, slightly shifted to lower wavenumber, typically a moderately intense peak at 2930–2900 cm^{-1} (asymmetric C–H stretch) and a weaker peak at ~2850 cm^{-1} (symmetric C–H stretch) (*18*). Thus the ν(C–H) region in the first spectrum could either be due to CH_3 groups only, with an overtone component at 2950 cm^{-1} (as for *t*-BuOH on aerosil, Fig. 2b), or the central component could arise from asymmetric C–H vibrations in CH_2 groups, the weaker peak from symmetric C–H vibrations being obscured by the stronger peak from C–H vibrations in CH_3 groups. Since the water peak shows that 50% reaction has already taken place, it seems very likely that the growth of the central component arises from CH_2 groups in the reaction products and the shift in peak positions with time merely reflects the further course of reaction. A similar increase in CH_2 concentration (as determined from analysis of the ν(C–H) region) has recently been reported (*25*) for the reaction of propan-2-ol on H-ZSM-5.

As time goes on, the central component increases relative to the 2980/2960 cm^{-1} peak paralleling the decrease of the 1375 cm^{-1} peak in the C–H deformation region. This shows the increase in concentration of CH_2 groups at the expense of $(CH_3)_3C$- groups during reaction. We thus differ from

Aronson *et al.* who interpret their spectroscopic data as evidence for the presence of *tert*-butyl carbonium ions (*8*) or silyl *tert*-butyl ether (*10*) as prevailing intermediates in the dehydration of *tert*-butanol.

While the change in $[CH_3]/[CH_2]$ accompanying dehydration makes it unlikely that *t*-butyl species are present to any great extent, it does not allow one to distinguish immediately between other adsorbed butyl isomers and adsorbed oligomers. However, we introduce the equivalent of 1 alcohol molecule for every zeolite OH group, i.e., [ROH] : [ZOH] = 1. Thus if all the organic species are present as simple ZO-butyl groups, then there will be no free zeolite OH groups. If adsorbed oligomers are formed, then some of these zeolite OH groups will become vacant. Let us consider further the spectral regions involving the OH-groups. As described in Section 3.1, at room temperature when we have mostly adsorbed alcohol (and only a small degree of reaction), we observe two broad component peaks at ~2450 and ~1500 cm^{-1} arising from zeolite OH-groups interacting with alcohol. The changes in these regions at 60°C, where reaction takes place rapidly, are shown in Fig. 4. As time increases, the broad component at ~1500 cm^{-1} disappears, while the broad peak at ~2450 cm^{-1} shifts to the left to a new sharper maximum. There is an accompanying change in the 3500–3700 cm^{-1} region, with the growth of a peak at ~3690 cm^{-1}. These final peak positions correspond to those observed for water adsorbed on H-ZSM-5, as reported elsewhere (*16, 25*), where with a water to zeolite OH-group ratio $[H_2O]/[ZOH]$ of $<1:1$, peaks are observed at ~3690 cm^{-1} corresponding to OH vibrations in water molecules, two broad peaks at ~2890 and ~2450 cm^{-1} for zeolite OH-groups interacting with adsorbed water, and a water deformation peak at 1640 cm^{-1}. In our spectra, the 2890 cm^{-1} region is obscured by the much stronger ν(C–H) bands, but the remaining peaks are observed. Thus in the course of reaction, we see a change from a zeolite with its acid OH-groups associated with alcohol molecules to ones associated with water molecules.

Thus during the course of reaction, at least some of the zeolite OH groups have been freed of adsorbed butyl. The only possibility (since no desorption of organic product takes place) seems to be that the butyl intermediate desorbs and reacts with a neighboring adsorbed butyl, forming an adsorbed oligomer on that active site; meanwhile, the thus vacated ZOH-group is able to interact with a water molecule, giving rise to the observed spectrum. The possibility that a substantial fraction of the butyl intermediate becomes adsorbed on Lewis acid sites, thus liberating zeolite OH groups, can be excluded because the concentration of Lewis acid sites in sample 2 was shown in Ref. (*16*) to be much smaller than that of OH-groups.

Thus in the spectra in Fig. 4, we are able to follow the alcohol dehydration reaction by the growth of the water deformation peak, but the so-formed butene oligomerizes and remains adsorbed on the active centers. Various isomeric oligomers can in principle be formed. However, on the basis of the changes in the C–H stretching and deformation vibration regions as reaction proceeds, it seems very likely that the adsorbed oligomer is a linear C_8 species of the type $\nearrow$ $-O-(CH_2)_7-CH_3$. This conclusion is supported by the following observations. As reaction proceeds:

(1) $[(CH_3)_3C\text{-}]$ $\downarrow$ (since I_{1375} $\downarrow$)

(2) $[CH_2]$ $\uparrow$ (since I_{2940} $\uparrow$).

Furthermore, the ν(C–H) peak for CH_2 groups at 2940 cm^{-1} is intense at the end of reaction (see Fig. 4, 60°C), being slightly higher than the ν(C–H) peak for CH_3 groups at 2960 cm^{-1}. In contrast, for *n*-BuOH adsorbed on aerosil (with no reaction), the $\nu(CH_2)$ peak is significantly less intense than the $\nu(CH_3)$ peak, and this in the case where the molecule has $1CH_3 : 3CH_2$ (*26*). The nature of the C–H stretching region in an oligomer bound to the zeolite as $\nearrow$–O–R_n would not be expected to differ much from those in the OR-fragment of alcohol since while

the possible different electronegativity of the oxygen atom in the two cases might be expected to influence the first CH_2 group, its influence should progressively decrease for groups further away. Indeed, for OH vibrations in X_3C–OH and X_3C–CO–OH, it is found (*27*) that on substituting X = H by X = Cl, a small shift is observed in the frequency of the OH vibration; however, substitution in X_3C–CH_2–OH causes no change. Thus, comparing the spectra of the observed oligomer with that of *n*-butanol, it seems likely that the oligomer may have three or more CH_2 groups per CH_3. If the oligomer is a dimer (C_8 oligomer), this is only possible in the case of a linear $\nwarrow$ –O–$(CH_2)_7$–CH_3 species. One cannot exclude unambiguously further oligomerization of butene inside the ZSM-5 channels, giving C_{12} and higher oligomers. However, note that according to GC–MS studies it is mainly C_8 species that desorb into the gas phase on heating a H-ZSM-5 sample (on which previously butanol dehydration was carried out) at elevated temperatures. The suggested, preferred formation of linear rather than branched C_8 oligomers is understandable within the narrow confines of the ZSM-5 pores (~5.5Å diameter (*28*)) and agrees with ^{13}C NMR results reported in Ref. (*29*) for the study of olefin reactions in ZSM-5.

3.3.3 Dehydration as the rate-determining step. Thus dehydration of *t*-BuOH is accompanied by both isomerization and oligomerization of the so-formed butene fragments. The identical proportionality of $-\Delta D_{CH_3}$ and $+\Delta D_{H_2O}$ for all three temperatures (Fig. 5c) shows that a similar process of dehydration accompanied by isomerization and oligomerization to linear C_8 adsorbed species, takes place in all these cases.

From the data in Fig. 5a and 5b, it is possible to estimate the rate constants for dehydration and isomerization at 40 and 60°C. Thus, treating the data for the CH_3 and water curves as first-order exponentials (taken from the point at t_o, where adsorption is more or less complete, as judged by the intensity of the peak at 1460 cm^{-1}), we find that at a given reaction temperature, the rate constants for the decay of $(CH_3)_3C$-groups and water formation have the same value. These data can be explained if we assume that in the sequence of reactions—dehydration, isomerization (oligomerization)—the rate-determining step is dehydration. From the rate constants determined at 40 and 60°C, we can obtain an estimate for the activation energy for dehydration of 19 ± 3 kcal/mol. Thus the processes taking place are slow dehydration of alcohol, accompanied by fast isomerization and oligomerization to linear adsorbed C_8 species (and possibly higher oligomers):

$$k_{\text{isomerization}},\ k_{\text{oligomerization}} \gg k_{\text{dehydration}}$$

Rapid oligomerization is consistent with the recent results of Haw *et al.* (*14*) who observe that for the propene/H-Y system, oligomerization is considerably faster than desorption of propene from the active centers. Similarly literature data, e.g., Ref (*30*), suggest that butene oligomerizes on H-ZSM-5 under mild conditions. The decrease in CH_3 groups with time, as follows from the above discussion of the data (Figs. 4 and 5a, 5b), arise from isomerization, but since both isomerization and oligomerization are fast, we cannot determine whether they take place in a specific order.

3.4 GC Kinetic Studies

In Section 3.3, we reported on the reaction in a static IR cell, where all the products remain adsorbed on the zeolite. We have also studied the reaction at the same temperature of 60°C in a flow reactor, where products may desorb owing to the continuous flow of alcohol reagent, and are registered by on-line GC. Thus in the GC kinetic studies, we analyze the products that desorb; this is complementary to our IR studies, where we monitor adsorbed species. Typical results for GC kinetic studies of dehydration are shown in Fig. 6. The rate of evolution of water gradually grows to a steady-

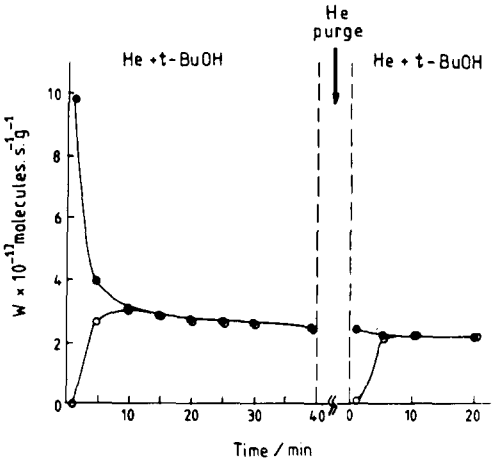

FIG. 6. Results of GC kinetic studies for *t*-BuOH dehydration on Na–H-ZSM-5, sample 2 at 60°C (flow reactor, [*t*-BuOH] = 1.1 mol%, m = 0.126 g, flow rate = 34.5 ml/min). At t = 40 min, the helium–alcohol mixture is replaced by pure helium, and reactant and products desorb (purging). After 15 min of purging, reactant mixture is again introduced and the kinetics of dehydration studied further. (●) butene, (○) water.

state value while the rate of evolution of butene is initially very high and then rapidly decreases to the steady-state rate. After 40 min on stream, the helium–alcohol mixture is replaced by pure helium, and unreacted alcohol together with butene and water, is desorbed. When the helium–alcohol reaction mixture is again passed through the sample, the rate of evolution of butene is initially identical to the steady-state rate observed prior to desorption with very slow deactivation with time; i.e., the initial high activity followed by rapid deactivation is no longer observed. This means that rapid deactivation is complete before purging.

From our IR studies at the same temperature, we see rapid formation of oligomers which remain adsorbed on the zeolite active centers. Thus it is the poisoning of the active sites inside the zeolite channels by adsorbed oligomers that can explain the rapid deactivation observed in the GC kinetic studies. The latter statement agrees with the fact that the characteristic time for catalyst deactivation in GC experiments (Fig. 6) is close to the characteristic time of oligomerization detected in the IR experiments (Fig. 5b). Note also that the amount of alcohol adsorbed on the catalyst in 1 min in GC experiments is indeed sufficient to block the OH-groups of the catalyst with oligomers formed upon alcohol dehydration. After this rapid deactivation to a steady-state level, only active sites located at the external surface of the ZSM-5 crystallites continue to work in *t*-BuOH dehydration. These active sites are deactivated more slowly than those located in the zeolite channels and they provide the same steady-state rates of butene and water evolution from *t*-BuOH both before and after purging. This very much resembles the results for *i*-BuOH dehydration on a more open system, namely amorphous aluminosilicate, where the absence of pore confinement reduced the probability of bimolecular butene collisions to such an extent that no deactivation from oligomerization was observed during reaction, and the steady-state activity before and after purging are identical (*15*).

Thus we conclude that the steady-state rate that we finally observe for *t*-BuOH dehydration arises from reaction occurring at the external surfaces of the zeolite crystallites, rather than in the internal volume. Under these conditions, the determination of reaction rate constants from kinetic data becomes a complicated problem involving the determination of the zeolite external surface area and the depth of the working layer. In addition, the reaction rate will strongly depend on crystallite size and crystallite size distribution, resulting in problems of reproducibility from sample to sample. As a result, we have not pursued these kinetic studies.

4. CONCLUSIONS

From IR studies, it has been possible to follow all the processes taking place in the *t*-BuOH/H-ZSM-5 system, namely, adsorption, dehydration, isomerization, and oligomerization. The IR studies of adsorption kinetics allow us to estimate the diffusion

coefficient for *t*-BuOH in ZSM-5 channels. The value obtained for diffusion in H-ZSM-5, namely 5×10^{-11} cm^2s^{-1} at 23°C, is reasonable in comparison with diffusion coefficient values in the literature for both smaller and larger molecules.

From IR studies of reaction at 40 and 60°C, we have identified the rapid formation of oligomers, which poison the active centers (zeolite OH-groups), remaining adsorbed on them most likely as linear C_8 species of the $\nearrow$–O–$(CH_2)_7$–CH_3 type. This conclusion agrees with the results of the GC kinetic studies, where we see high initial activity of H-ZSM-5 and its rapid deactivation. The IR results at 60°C show that the rate-determining step for all the reactions observed in the *t*-BuOH/H-ZSM-5 system is dehydration (with an activation energy of 19 ± 3 kcal/mol), with subsequent isomerization and oligomerization of the butyl species being considerably faster. The butene that is formed upon *t*-BuOH dehydration initially desorbs from the active site and then rapidly interacts with a neighboring adsorbed butyl species, resulting in the formation of adsorbed oligomers (mainly dimers). In addition, isomerization takes place, but since both isomerization and oligomerization are fast, we cannot on the basis of our data determine whether isomerization takes place prior to, simultaneously with, or after, oligomerization. The zeolite OH-groups vacated due to involvement of butene molecules in oligomerization, interact with water molecules formed as a result of dehydration.

Unfortunately, it is not possible to directly observe all the intermediate steps described above. We deduce the above sequence of events from the observation at 40 and 60°C of a growth in the peak for water and, simultaneously, a decrease in the number of $(CH_3)_3C$-groups, an increase in the number of CH_2 groups, and a change from the case where the zeolite OH-groups are interacting with organic species to one where at least some of them are interacting with water molecules. Similar results are observed at room temperature, but on a longer timescale.

Thus oligomers are the prevailing adsorbed species during the dehydration of *t*-BuOH on ZSM-5. Our conclusions therefore differ from those of Aronson *et al.* who interpret their spectroscopic data as evidence for stable *tert*-butyl carbonium ions (*8*) or *tert*-butyl silyl ether (*10*) intermediates for *t*-BuOH dehydration in H-ZSM-5.

ACKNOWLEDGMENTS

The authors thank Dr. V. N. Romannikov (Institute of Catalysis) for zeolite samples 4 and 5. One of us (C.W.) thanks the Royal Society and the USSR Academy of Sciences for a fellowship.

REFERENCES

1. Zamaraev, K. I., and Zhidomirov, G. M., *in* "Proc. 5th. Int. Symp. Homog. Heterog. Catal." (Yu. Yermakov and V. Likholobov, Eds), pp. 23–73. VNU Science, Netherlands, 1986.
2. Thomas, J. M., *Angew. Chem. Int. Ed. Eng.* **27,** 1673 (1988).
3. Breck, D. W., "Zeolite Molecular Sieves." Wiley-Interscience, New York, 1974.
4. Palekar, M. G., and Rajadhyaksha, R. A., *Catal. Rev. Chem. Eng.* **28,** 371 (1986).
5. Chang, C. D. *Catal. Rev. Sci. Eng.* **25,** 1 (1983).
6. Ono, Y., and Mori, T. J., *J. Chem. Soc. Faraday Trans. 1* **77,** 2209 (1981).
7. Forester, T. R., and Howe, R. F., *J. Amer. Chem. Soc.* **109,** 5076 (1987).
8. Aronson, M. T., Gorte, R. J., and Farneth, W. E., *J. Catal.* **105,** 455 (1987).
9. Bronniman, C. E., and Maciel, G. E., *J. Amer. Chem. Soc.* **108,** 7154 (1986).
10. Aronson, M. T., Gorte, R. J., Farneth, W. E., and White, D. J., *J. Amer. Chem. Soc.* **111,** 840 (1989).
11. Lombardo, E. A., Dereppe, J. M., Marcelin, G., and Hall, W. K., *J. Catal.* **114,** 167 (1988).
12. Sykes, P., "Mechanism of Reactions in Organic Chemistry." Longman, White Plains, NY, 1971.
13. Olah, G. A., DeMember, J. R., Commeryras, A., and Bribes, J. L., *J. Amer. Chem. Soc.* **93,** 459 (1971).
14. Haw, J. F., Richardson, B. R., Oshiro, I. S., Lazo, N. D., and Speed, J. A., *J. Amer. Chem. Soc.* **111,** 2052 (1989).
15. Makarova, M. A., Williams, C., Romannikov, V. N., Thomas, J. M., and Zamaraev, K. I., *J. Chem. Soc. Faraday Trans. 1* **86,** 581 (1990).
16. Williams, C., Makarova, M. A., Malysheva, L. V., Paukshtis, E. A., Talsi, E. P., Thomas, J. M., and

Zamaraev, K. I., *J. Chem. Soc. Faraday Trans.*, **86,** 3473 (1990).
17. Romannikov, V. N., Mastikhin, V. M., Hočevar, S., and Drzaj, B., *Zeolites* **3,** 311 (1983).
18. Sverdlov, L. M., Kovner, M. A., and Krainer, E. P., "Vibration Spectra of Polyatomic Molecules." Nauka, Moscow, 1970.
19. Kiselev, A. V., and Lygin, V. I., "IR Spectra of Surface Compounds and Adsorbed Species." Nauka, Moscow, 1972.
20. Jacobs, P. A., and von Ballmoos, R., *J. Phys. Chem.* **86,** 3050 (1982).
21. Sokolov, N. D., "The Hydrogen Bond." Nauka, Moscow, 1981.
22. Caro, J., Hočevar, S., Karger, J., and Riekert, L., *Zeolites* **6,** 213 (1986).
23. Karger, J., and Ruthven, D. M., *Zeolites* **9,** 267 (1989).
24. Choudhary, V. R., and Akolekar, D. P., *J. Catal.* **117,** 542 (1989).
25. Jentys, A., Warecka, G., and Lercher, J. A., *J. Mol. Catal.* **51,** 309 (1989).
26. Makarova, M. A., and Williams, C., unpublished results.
27. (a) Bellamy, L. J., "Advances in Infrared Group Frequencies." Chapman and Hall, London, 1968. (b) Rossarre, J., Gallas, J. P., Benet, C., and Romanet, R., *J. Chim. Phys.* **74,** 197 (1977).
28. Kokotailo, G. T., Lawton, S. L., Olson, D. H., and Meier, W. M., *Nature (London)* **272,** 437 (1978).
29. van den Berg, J. P., Wolthuizen, J. P., Clague, A. D. H., Hays, G. R., Huis, R., and van Hooff, J. H. C., *J. Catal.* **80,** 130 (1983).
30. Irving, J. D. N., Leach, H. F., Whan, D. A. and Spencer, M. S. *J. Chem. Res. Synop.*, 66 (1982).